

I.N. Nurgaliev

Institute of Polymer Chemistry and Physics, Tashkent, Uzbekistan
(*Corresponding author's e-mail: ilnarvodnik@gmail.com)

DFT Study of Chitosan Ascorbate Nanoparticles Structure

In recent years, use of chitosan (CS) nanoparticles as nanocarriers has received much attention due to their biodegradability, biocompatibility, and non-toxicity. CS nanoparticles containing drugs, flavors, enzymes, and antimicrobial agents can maintain their activity. Such nanoparticles can stimulate the stabilization of ascorbic acid (AA) and improve controlled release. This study investigates the interaction of CS monomer with AA and sodium triphosphate (TPP) using density functional theory (DFT) during the formation of chitosan ascorbate (CA) nanostructure (CAN). Based on existing results, the formation of the CS monomer from the complexes occurs due to the donor-acceptor interaction, which is energetically favorable in all considered interactions according to the calculations. At close range, proton transfer has been identified with interaction energies, namely CS-AA (-6.82 kcal/mol), CS-TPP (-4.56 kcal/mol) in the aqueous phase, which indicates that in the process of CAN formation, in most cases, the formation of a donor-acceptor bond occurs between the amino groups of CS with the enol group of AA and the relative coordination of CS with TPP. The introduction of the aqueous phase led to a drop in the interaction energy. Based on our results for the linking types (interaction energies), we propose a simple mechanism for their impact on the CAN formation process.

Keywords: chitosan, ascorbic acid, sodium triphosphate, chitosan ascorbate, nanoparticles, modeling.

Introduction

Chitosan (CS) is a polysaccharide consisting of N-acetyl-D-glucosamine and D-glucosamine linked by the β -(1 \rightarrow 4) bonds [1]. CS is recognized as a natural biopolymer that includes numerous functional groups, such as the amine (NH_2) and hydroxyl (OH), and it is made via the deacetylation of chitin. Ascorbic acid (AA) plays an important role in metabolism, acting as both an acceptor and a proton donor in enzymatic systems, due to the mobility of hydrogen atoms in enol hydroxyls at C-3 ($\text{pK}_a = 4.2$) and C-2 ($\text{pK}_a = 11.6$) [2]. CS is a biodegradable, non-toxic biopolymer; it has properties that stimulate plant growth and inhibit phytopathogenic fungi; it possesses immunological modulation and antiviral efficacy; it has a wide range of applications, particularly in anti-coronavirus applications [3, 4]. Water-soluble environmentally safe derivatives of CS, in particular, chitosan ascorbate (CA) are of great interest in the world. A wide possibility of CS modification allows one to obtain its water-soluble derivatives, among which CA is of special interest, that exhibit pronounced bioactivity in the growth and development of plants [5, 6].

CA is an organic salt formed by the reaction of CS with AA and it shows a more pH-independent solubility profile, thus providing more flexibility in biomaterial processing and fabrication. CA is synthesized by the direct reaction of CS and AA in water (Figure 1) [7–9].

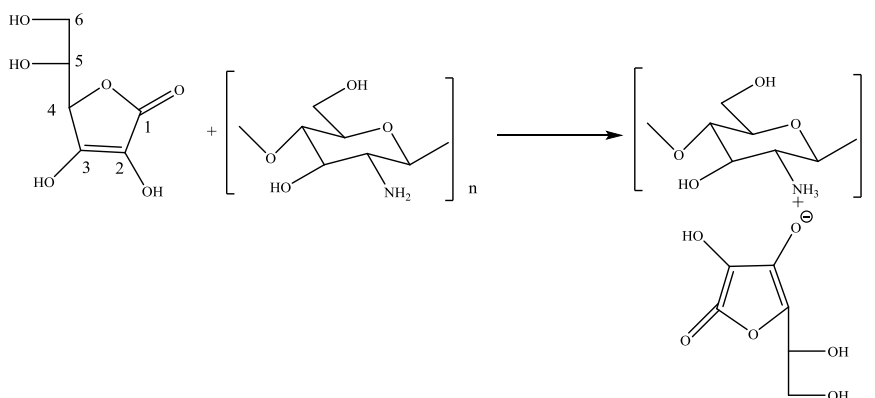


Figure 1. Mechanism of interaction between CS and AA

The product formed is the CS-AA complex, which is different from the CS-AA mixture in that no protonation of CS occurs in the latter [10]. AA presents several electrophilic groups. It contains four hydroxyl groups in positions 2, 3, 5, and 6 with different acidities allowing acid-base reactions. The -OH in position 3 is more acidic one ($pK_a = 4.2$), while the hydroxyl in position 2 has a pK_a of 11.6, and those in positions 5 and 6 behave as secondary and primary alcohol ($pK_a \approx 17$ and 16, respectively) [11]. The acidic hydroxyl in position 3 of AA was expected to react with the amino group of CS, converting it into ammonium ions. The FT-IR spectra demonstrate the formation of complex between CS and AA [11]. The peak at 1754.4 cm^{-1} , which was the stretching vibration of lactone C=O forming intramolecular H-bond in AA, was shifted to 1720.8 cm^{-1} at a reduced intensity. It could be seen that new absorption band characteristic of bending vibration of $-\text{NH}_3^+$ appeared at 1616.1 cm^{-1} . This result suggested that the $-\text{NH}_2$ groups on the CS chains were protonated by the H^+ supplied by AA [12]. The decrease of peak at 3428.2 cm^{-1} indicated the reduction of free $-\text{NH}_2$ groups after the formation of CS-AA complex [13].

Despite the ubiquitous presence of these interactions in chemical processes, few DFT studies on these systems exist in the literature [14–16]. There are few works on determining the activation energy of the formation reaction and modeling the structure of chitosan ascorbate nanostructure (CAN). Complexes of CS with organic acids are obtained mainly by the method of ionotropic gelation, coacervation precipitation, and ultrasonic dispersion [10, 13, 17–22]. However, there are advantages and disadvantages of the above methods for obtaining nanoparticles. If the method of ionotropic gelation is considered technologically acceptable and no additional purification is required for a long time of the final products, then by the method of coacervation precipitation, side compounds are formed due to ions of inorganic salts. When obtaining nanoparticles of CS derivatives by ultrasonic dispersion, it is impossible to control the process, which in turn makes it difficult to control their characteristics.

Thus, the formation of nanoparticles is a multifactorial process that depends on the ratio, concentration of components and solution pH [7–9]. The method of ionic gelation is the most well-known one among the methods for obtaining CAN. However, in studies when obtaining CAN, deprotonation of CS is not carried out; this stage plays a special role in the formation of a donor-acceptor bond between the amino group of CS and the enol group of AA [10, 17–20]. Since without deprotonation of the amino groups of CS, an excess amount of AA in the reaction system increases, this makes it impossible to analyze the properties of the final product [18, 21]. Therefore, in recent works, there was improvement in the method with the inclusion of the step of deprotonation of CS amino groups [7, 19, 22]. Based on the obtained deprotonated CS with varying pH and the ratio of the reaction components and the TPP stabilizer, it is possible to control the size of the resulting nanoparticles of CS derivatives with organic acids, including AA. Nano derivatives of CS with AA have growth-regulating, antimicrobial, and wound-healing properties; solutions of nano derivatives of CS are environmentally safe and low-toxic [10, 19, 20]. It is noted in the literature that the reaction of formation of CS nanoascorbate occurs due to the donor-acceptor bond. The ratio of components and solution pH play a special role in this process [24, 25]. Aqueous solutions of AA are used to obtain water-soluble nano derivatives of CS. The formation of CAN is carried out by varying the solution pH in the range from 4 to 5.5 [19, 26]. Physicochemical properties of biologically active nanostructured complexes of CS with AA are poorly studied, and theoretical works on the formation of CAN have not been found [3, 10, 21–26].

Computational research effectively helps to understand the nature of these interactions and it is less time-consuming and considerably less expensive than experimental analyses. Thus, the objective of the current work is to investigate the interaction of CS with AA and TPP using the DFT method to be a primer for understanding the CAN formation, as well as for theoretical validation of literature experimental results. The optimized geometry, frontier molecular orbitals (FMOs) and details of quantum molecular descriptors were calculated.

Experimental

Computational methods

In this work, we carry out quantum theoretical calculations and optimized the model of interaction of monomer form of CS with AA and TPP structure at the B3LYP/6-31++G(d,p) level (DFT) [28–30] by the GAUSSIAN09 program package [27] and calculate its properties. The charge state of atoms is calculated, diagrams of boundary molecular orbitals are constructed: the highest occupied (HOMO) and lowest free (LUMO) molecular orbitals, and their energies are determined. In DFT reactivity descriptors, such as global hardness (η) is determined using finite difference approximation and Koopmans' theorem [31] as:

$$\eta = \frac{1}{2} \left(\frac{\partial^2 E}{\partial N^2} \right)_{v(\bar{r})} = \frac{1}{2} \left(\frac{\partial \mu}{\partial N} \right)_{v(\bar{r})}, \quad (1)$$

where E — the energy and N is the number of electrons in the electronic system at constant external potential (v), μ — the chemical potential:

$$(\mu = 1/2(E_{\text{HOMO}} + E_{\text{LUMO}})). \quad (2)$$

η is calculated in terms of ionization potential ($-E_{\text{HOMO}}$) and electron affinity ($-E_{\text{LUMO}}$) using the following formulae:

$$\eta = (E_{\text{LUMO}} - E_{\text{HOMO}}) / 2. \quad (3)$$

Free energy of solvation is computed by equation:

$$\Delta G_{\text{sol}} = G_{\text{solvent}} - G_{\text{gas}}, \quad (4)$$

that numerical values obtained by using Solvation Model of Density (SMD) [32]. The interaction energy (ΔE_{int}) between CS and AA, TPP is calculated using super molecular approach

$$\Delta E_{\text{int}} = (E_{\text{CAN}}) - (E_{\text{CS}} + E_{\text{AA}} + E_{\text{TPP}}), \quad (5)$$

where E_{CAN} — the energy of the CAN adduct; E_{CS} — the energy of CS; E_{AA} — the energy of the AA and, E_{TPP} — the energy of the TPP.

The energy difference was taken before or after the proton transfer, for example, between CS^+ and AA^- , TPP^- ions. Global reactivity descriptor, namely the global hardness is calculated using global hardness values. To quantify the reactivity in aqueous phase, solvation energies are calculated using self-consistent reaction field theory through the Polarizable Continuum Model (PCM) [33, 34]. In calculating interaction energy, basis set superposition error (BSSE) is considered by using counterpoise = N [35, 36].

Results and Discussion

Model structures were built for simulating the possibility of CAN structure. Models were presented as one unit of CS representing the main model molecule. The interactions between CS molecules with AA and TPP can occur, as observed in the results addressed so far, by donor-acceptor interaction involving $-\text{OH}$ or $-\text{NH}_3^+$ groups from CS. To evaluate this interaction, as well as describe some quantum properties of the CAN model, which are scarce in the literature, a computational study was realized. FMOs were calculated to gain a deeper insight into the quantum properties of the CAN model. The FMOs results provide knowledge about the energy gap and electronic properties between the HOMO and LUMO of the CS-AA and CS-TPP interactions. The HOMO can be considered the outermost orbital containing electrons, which characterizes the ability of electron donor, while LUMO is considered the innermost orbital containing free places to accept electrons [37].

The optimized CS-AA and CS-TPP structures have been calculated by B3LYP/6-31++G(d,p), the level of theory is shown in Figure 2. The distance between the hydrogen atom of the CS amino group and the oxygen atoms of AA and TPP is in the range of 1.52–1.98 Å, which is typical for donor-acceptor interaction and thus establishes the fact that the product of the interaction of one monomer units of CS with AA and TPP are held together by a donor-acceptor mechanism. A bond is formed in the case of interaction of CS with AA ($r = 1.60$ Å, $\theta = 171.1^\circ$), as well as CS with TPP ($r = 1.53$ Å, $\theta = 178.7^\circ$).

According to calculations, the hydroxyl group of AA in position 3 (C3-O) will react with the amino group of CS, converting it into ammonium ions. The enol group of AA reacts with the $-\text{NH}_3^+$ group of CS with the formation of oxoammonium (Figure 1), due to the donor-acceptor interaction, a CS complex is formed. Amino groups in CS chains can be protonated by AA to form a positively charged water-soluble polysaccharide. CA in an acidic solution undergoes ionic gelation and forms CAN particles with a crosslinking agent added to the solution. Crosslinking occurs due to electrostatic interaction between positively charged amino groups of CS and negatively charged oxygen atoms of TPP. The size of the formed particle mainly depends on the concentration of the acid (acetic acid) and deacetylation degree (DD) of CS [24, 25]. CS with a higher DD is characterized by a large number of effective binding points, i.e., amino groups that are protonated in an acidic solution [7]. Moreover, in an acidic solution, the degree of protonation of amino groups in the chains of CS increases, which, as a result, increases the ability to form cross-links with TPP. The binding of TPP to the polymer occurs until the degree of binding that also depends on the concentration of TPP, decreases, which eventually leads to the formation of smaller nanoparticle sizes, and after saturation, excessive binding will lead to the formation of aggregates, resulting in large particle size [8–10, 25, 26].

The magnitude of interaction is of paramount importance for nanostructure stabilization. A strong or weak interaction, both are equally unfavorable for biological activity. The weak interaction is unfavorable for the stability of such nanoparticles. For exhibiting biological activity, a suitable interaction energy range is 10 kcal/mol [10, 21–23]. To examine the magnitude of the interaction between CS and AA, TPP, we estimated the interaction energy using a supermolecular approach. Initially, we calculated the interaction energies (ΔE_{int}) in the gas phase and then observed the impact of aqueous phase on the interaction energy (Table 1). In the gas phase, ΔE_{int} is observed to be high and the order is CS-AA (–68.76 kcal/mol) > CS-TPP (–64.58 kcal). The observed trend does not corroborate with that predicted from the bond angle (θ) values in donor-acceptor bonding. This indicates that the bond angle in donor-acceptor bonding is not the sole criterion that governs the interaction energies between two compounds.

During CAN delivery, transfection of nanoparticles takes place through a complex physiological medium, whose main constituent is water [13, 17]. Cationic charge of CS attracts a large scale of solvation and thereby enhances stability of CS. Therefore, incorporation of aqueous phase produces a spiky fall in interaction energies as compared to the gas phase. The aqueous phase ΔE_{int} (using PCM model) values of interactions are in the order: CS-AA (–13.67 kcal/mol) > CS-TPP (–11.2 kcal/mol). We have further calculated the free energy of solvation (ΔG_{sol}) (using SMD solvation model) of the chosen CS-AA and CS-TPP. The order is observed to be: CS-AA (–66.32 kcal/mol) > CS-TPP (–62.45 kcal/mol), higher values are due to positive charge inherent in the interactions.

Quantum chemical methods are important for obtaining information about the molecular structure and the interaction behavior. In the synergic effect of interactions of the type CS + nucleophile(AA,TPP) = CAN, intermolecular donor-acceptor interaction formation is favored when the HOMO of the CAN has lower energy than the HOMO of CS or LUMO of AA and TPP [33]. Hence, we have calculated the energy separation $\Delta E_{gas, aq} = (E_{HOMO(gas, aq)}^{CAN} - E_{HOMO(gas, aq)}^{nucleophile(AA, TPP)})$. It is evident from Table 1 that $E_{HOMO,CAN}$ is lower than $E_{HOMO, nucleophile(AA,TPP)}$ and $E_{LUMO,CS}$. This indicates that the formation of donor-acceptor interactions is beneficial in all considered interactions from the HOMO-LUMO energy data. Figure 2 illustrates the mapping of HOMO and LUMO orbitals.

Earlier, [38–40] reported a correlation between the energy separation $\Delta E_{gas, aq}$ values and interaction energy, ΔE_{int} which showed an increase in interaction energy with an increment in ΔE values (ΔE_{int} against $\Delta E_{gas, aq}$). Here we observe high ΔE_{gas} values (–51.49 kcal/mol to –72.42 kcal/mol) for interactions in the gas phase in compliance with high magnitude of the gas phase interaction energies (–64.58 kcal/mol to –68.76 kcal/mol). Incorporation of aqueous phase lowers ΔE_{aq} values (–4.56 kcal/mol to –6.82 kcal/mol) along with a fall in interaction energy (–11.2 kcal/mol to –13.67 kcal/mol). However, no linear relationship between ΔE and ΔE_{int} is observed. Apart from ΔE values, shape of the LUMO of the donor and HOMO of the acceptor is also important. Figure 2 reveals that HOMO and LUMO of CS-TPP are localized over the $-\text{NH}_3^+$ group, and this facilitates the $-\text{NH}_3^+$ group to participate in donor-acceptor interactions. Moreover, LUMO of CS-AA is spreading over the O atoms of AA and TPP, which makes them hydrogen acceptor during donor-acceptor bonding formation.

Gas phase BSSE corrected ΔE_{int} calculated values of the chosen adducts are presented in Table 1. We observe high ΔE_{gas} values for CS-AA and CS-TPP interactions (–72.42 kcal/mol and –51.49 kcal/mol) in the gas phase. Incorporation of aqueous phase lowers ΔE_{aq} values (–6.82 kcal/mol and –4.56 kcal/mol), respectively. However, no linear relationship between ΔE and ΔE_{int} is observed. Apart from ΔE values, shape of the LUMO of the donor and HOMO of the acceptor is also important. Figure 2 reveals that HOMO of CS-AA is localized over the $-\text{NH}_3^+$ group, whereas the LUMO orbital resides on the lactone-ring of AA molecule, which makes them hydrogen acceptor during donor-acceptor bonding formation. The LUMO of CS-TPP is localized over the TPP molecule, HOMO is slightly spreading over on $-\text{NH}_3^+$ group of CS molecule.

Table 1

Calculated parameters (in kcal/mol) of the studied systems

Structure	ΔE_{int} (BSSE correct)	ΔE_{int}	ΔE_{int} (using PCM model)	ΔG_{sol} (using SMD solvation model)	ΔE_{gas}	ΔE_{aq}	ΔG_{gas}	ΔG_{aq}	η , gas phase	η , aqueous phase
CS-AA	–68.76	–70.21	–13.67	–66.32	–72.42	–6.82	–40.34	–3.37	63.7	60.3
CS-TPP	–64.58	–66.32	–11.2	–62.45	–51.49	–4.56	–41.35	–3.08	49.7	59.3

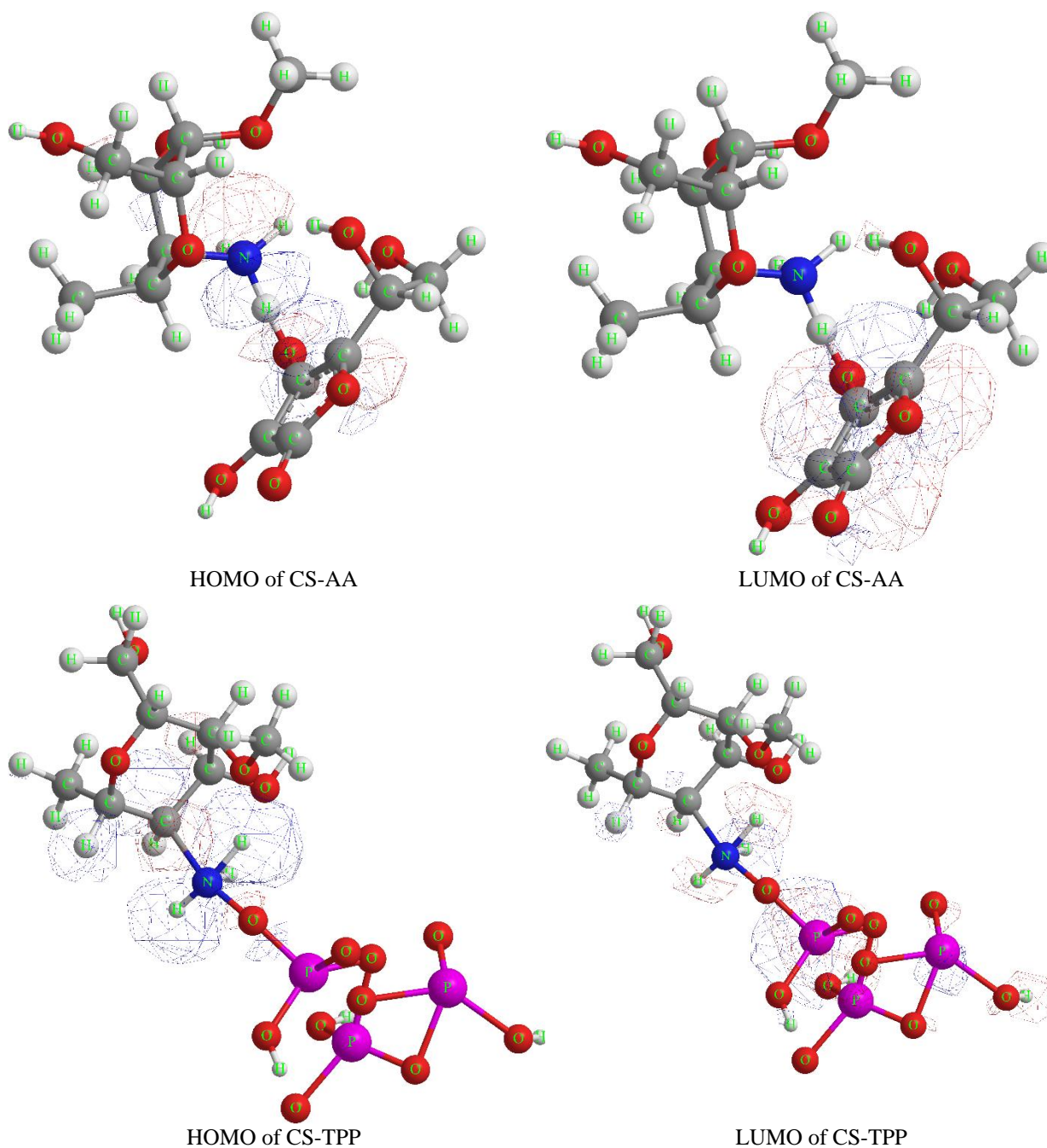


Figure 2. Molecular orbital surfaces for HOMO and LUMO of CS-AA and CS-TPP

We performed thermochemical analysis, to examine the thermodynamic driving force involved in the interactions. The ΔG_{gas} and ΔG_{aq} values are presented in Table 1. It is evident that in the gas phase, free energy favors interactions. In the gas phase, ΔG values follow the order CS-AA (-40.34 kcal/mol) < CS-TPP (-41.35 kcal/mol). However, a spiky fall in ΔG values is observed in the aqueous phase exhibiting negative ΔG_{aq} values. ΔG_{aq} values are in the order: CS-AA (-3.37 kcal/mol) < CS-TPP (-3.08 kcal/mol). This demonstrates the influence of solvent polarity on the parameter and the large role of thermodynamic driving forces in the aqueous phase, also for other systems [16, 38–44].

In accordance with the literature data [17–19] and the data of the calculation results, we proposed a model of CAN, which is represented in Figure 3.

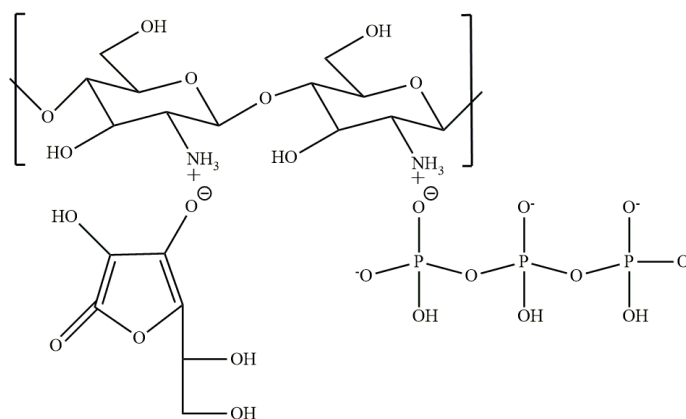


Figure 3. Interaction mechanism of CS-AA-TPP

Stability of the CAN can be monitored in terms of global hardness, in both gas and aqueous phases. The result in Table 1 elucidates the gas and aqueous phase global hardness of CS-AA and CS-TPP. Global hardness of the interaction values in both phases is comparable but slightly lower values in the aqueous phase imply that they are less stable in the aqueous phase.

Conclusions

In the present study, the electronic structure of interaction of CS to interact with AA and TPP has been analyzed using the DFT calculations B3LYP/6-31++G(d,p). The DFT results establish the existence of strong donor-acceptor interactions between CS and the AA and TPP in the gas phase. The introduction of the aqueous phase led to a drop in the interaction energy. The results show that the HOMO of CS-AA and CS-TPP is localized over the $-NH_3^+$ group, whereas the LUMO orbital resides on the lactone-ring of AA molecule, which makes them hydrogen acceptor during donor-acceptor bonding formation. The LUMO of CS-TPP is localized over the TPP molecule. According to the frontier orbital analysis, the AA had the greatest contributions to HOMO and LUMO. In addition, an increase in the acidity of the medium, the concentration of AA and TPP as well as the DD of CS can be considered as a tool for obtaining nanoparticles of various sizes. CS nanoparticles can protect AA from degradation and improve the stability of AA. CS-based drug delivery systems can be improved by adopting different theoretical and synthetic techniques and selecting appropriate process parameters and functional properties.

References

- Miguel, J., Radhouani, O.H., & Reis, R.L. (2021). Chitosan. *Chapter in book: Polysaccharides of Microbial Origin*, Springer, Cham, 1–18. https://doi.org/10.1007/978-3-030-35734-4_14-1
- Evdokimov, I.A., Alieva, L. R., Varlamov, V.P., Kharitonov, V.D., Butkevich, T.V., & Kurchenko, V.P. (2015). Usage of chitosan in dairy products production. *Foods and Raw Materials*, 3(2), 29–39. <https://doi.org/10.12737/13117>
- Safer, A.-M., & Leporatti, S. (2021). Chitosan nanoparticles for antiviral drug delivery: A Novel Route for COVID-19 Treatment. *International Journal of Nanomedicine*, 16, 8141–8158. <https://doi.org/10.2147/IJN.S332385>
- Mondal, A., Dhar, A.K., Banerjee, S., Hasnain, Md S., & Nayak, A.K. (2022). Antimicrobial uses of chitosan. *Chapter in book: Chitosan in Biomedical Application*, Academic Press, Elsevier, 13–36. <https://doi.org/10.1016/B978-0-12-821058-1.00009-5>
- Balusamy, S.R., Rahimi, S., Sukweenadhi, J., Sunderraj, S., Shanmugam, R., Thangavelu, L., Mijakovic, I., & Perumalsamy, H. (2022). Chitosan, chitosan nanoparticles and modified chitosan biomaterials, a potential tool to combat salinity stress in plants. *Carbohydrate Polymers*, 284(2), 19189. <https://doi.org/10.1016/j.carbpol.2022.119189>
- Gayen, K., Pabale, S., Shirolka Sarkar, S., & Roychowdhury, S. (2022). Chitosan biomaterials: Natural resources for dentistry. *International Journal of Oral Health Sciences*, 11(2), 75–79. https://doi.org/10.4103/ijohs.ijohs_18_21
- Sekar, V., Rajendran, K., Vallinayagam, S., Deepak, V., & Mahadevan, S. (2018). Synthesis and characterization of chitosan ascorbate nanoparticles for therapeutic inhibition for cervical cancer and their in silico modeling. *Journal of Industrial and Engineering Chemistry*, 62, 239–249. <https://doi.org/10.1016/j.jiec.2018.01.001>
- Rossi, S., Marciello, M., Sandri, G., Bonferoni, M.C., Ferrari, F., & Caramella, C. (2008). Chitosan ascorbate: a chitosan salt with improved penetration enhancement properties. *Pharmaceutical Development and Technology*, 13, 513–521. <https://doi.org/10.1080/10837450802288865>

- 9 Elbarbary, A.M., Shafik, H.M., Ebeid, N.H., Ayoub, S.M., & Othman S.H. (2015). Iodine-125 chitosan-vitamin C complex: preparation, characterization and application. *Radiochimica Acta*, 103, 663–671. <https://doi.org/10.1515/ract-2014-2303>
- 10 Tian, X.L., Tian, D.F., Wang, Z.Y., & Mo, F.K. (2009). Synthesis and evaluation of chitosan-vitamin C complex. *Indian Journal of Pharmaceutical Sciences*, 71(4), 371–376. <https://doi.org/10.4103/0250-474X.57284>
- 11 Capuzzi, G., Nostro, P.L., Kulkarni, K., & Fernandez, J.E. (1996). Mixtures of stearyl- 6-O-ascorbic acid and α -tocopherol: A monolayer study at the gas/water interface. *Langmuir*, 12, 3957–3963. <https://doi.org/10.1021/la960001y>
- 12 Zheng, C., Yan, X., Si, J.G., Meng, Y., Qi, Z., & Tao, Z. (2008). Ionic interactions between sulfuric acid and chitosan membranes. *Carbohydrate polymers*, 73, 111–116. <https://doi.org/10.1016/j.carbpol.2007.11.009>
- 13 Mao, S.R., Shuai, X.T., Unger, F., Simona, M., Bi, D.Z., & Kissel, T. (2004). The depolymerization of chitosan: Effects on physicochemical and biological properties. *International Journal of Pharmaceutics*, 281(1-2), 45–54. <https://doi.org/10.1016/j.ijpharm.2004.05.019>
- 14 Pacheco-García, P.F., Perez-Gonzalez, A., Ramos-Flores, A., Flores-Gonzalez, L.A., Lopez-Oglesby, J.M., & Gonzalez-Perez, M. (2017). Experimental study and calculation of the electron transfer coefficients on the dissolution behavior of chitosan in organic acids. *International Journal of Advanced Engineering, Management and Science*, 3(6), 703–709. <https://dx.doi.org/10.24001/ijaems.3.6.14>
- 15 An, X., Kang, Y., & Li, G. (2019). The interaction between chitosan and tannic acid calculated based on the density functional theory. *Chemical Physics*, 520, 100–107. <https://doi.org/10.1016/j.chemphys.2018.12.009>
- 16 Siahaan, P., Sasongko, N.A., Lusiana, R.A., Prasasty, V.D., & Martoprawiro, M.A. (2021). The validation of molecular interaction among dimer chitosan with urea and creatinine using density functional theory: In application for hemodialysis membrane. *International Journal of Biological Macromolecules*, 168, 339–349. <https://doi.org/10.1016/j.ijbiomac.2020.12.052>
- 17 Deshmukh, A.R., & Kim, B.S. (2019). Chitosan-vitamin C nanoparticles. *Korean Society for Biotechnology and Bioengineering Journal*, 34(4), 221–232. <https://doi.org/10.7841/ksbbj.2019.34.4.221>
- 18 Augustine, R., Dan, P., Schlachet, I., Rouxel, D., Menu, P., & Sosnik, A. (2019). Chitosan ascorbate hydrogel improves water uptake capacity and cell adhesion of electrospun poly(epsilon-caprolactone) membranes. *International Journal of Pharmaceutics*, 559(25), 420–426. <https://doi.org/10.1016/j.ijpharm.2019.01.063>
- 19 Othman, N., Masarudin, M.J., Kuen, C.Y., Dasuan, N.A., Abdullah, L.Ch., & Jamil, Md. S.N.A. (2018). Synthesis and optimization of chitosan nanoparticles loaded with L-ascorbic acid and thymoquinone. *Nanomaterials*, 8(11), 920. <https://doi.org/10.3390/nano8110920>
- 20 Liu, J., Pu, H., Zhang, X., Xiao, L., Kan, J., & Jin, Ch. (2018). Effects of ascorbate and hydroxyl radical degradations on the structural, physicochemical, antioxidant and film forming properties of chitosan. *International Journal of Biological Macromolecules*, 114, 1086–1093. <https://doi.org/10.1016/j.ijbiomac.2018.04.021>
- 21 Baek, J., Ramasamy, M., Carly Willis, N., Kim, D.S., Anderson, W.A., & Tam, K.C. (2021). Encapsulation and controlled release of vitamin C in modified cellulose nanocrystal/chitosan nanocapsules. *Current Research in Food Science*, 4, 215–223. <https://doi.org/10.1016/j.crfs.2021.03.010>
- 22 Alishahi, A., Mirvaghefi, A., Tehrani, M.R., Farahmand, H., Shojaosadati, S.A., Dorkoosh, F.A., & Elsabee, M.Z. (2011). Shelf life and delivery enhancement of vitamin C using chitosan nanoparticles. *Food Chemistry*, 126, 935–940. <https://doi.org/10.1016/j.foodchem.2010.11.086>
- 23 Esraa Abu El, Q.M., Mohamed, A.S., Fahmy, S.R., Soliman, A.M., & Gaafar, Kh. (2021). Silver/chitosan/ascorbic acid nanocomposites ameliorate diabetic nephropathy in the model of type 1 diabetes. *GSC Biological and Pharmaceutical Sciences*, 16(03), 091–102. <https://doi.org/10.30574/gscbps.2021.16.3.0263>
- 24 Pirmiyazov, K.K., & Rashidova, S.Sh. (2020a). Synthesis of ascorbate and nanoascorbate of chitosan and their biologically active properties. *Science and innovative development*, 5, 47–62.
- 25 Pirmiyazov, K.K., & Rashidova, S.Sh. (2020b). Study of the kinetics of Bombyx mori chitosan ascorbate formation. *Bulletin of the University of Karaganda – Chemistry*, 99(3), 38–43. <https://doi.org/10.31489/2020Ch3/38-43>.
- 26 Rossi, S., Vigani, B., Puccio, A., Bonferoni, M.C., Sandri, G., & Ferrari, F. (2017). Chitosan ascorbate nanoparticles for the vaginal delivery of antibiotic drugs in atrophic vaginitis. *Marine Drugs*, 15(10), 319. <https://doi.org/10.3390/md15100319>.
- 27 Frisch, M.J., Trucks, G.W., Schlegel, H.B., Scuseria, G.E., Robb, M.A., Cheeseman, J.R., Scalmani, G., Barone, V., Mennucci, B., Petersson, G.A., et al. (2010). Gaussian, Inc., Wallingford CT.
- 28 Becke, A.D. (1993). Density-functional thermochemistry. III. The role of exact exchange. *The Journal of Chemical Physics*, 98, 5648–5652. <https://doi.org/10.1063/1.464913>.
- 29 Lee, C., Yang, W., & Parr, R.G. (1988). Development of the Colle-Salvetti correlation-energy formula into a functional of the electron density. *Physical Review B*, 37, 785–789. <https://doi.org/10.1103/physrevb.37.785>.
- 30 Miehlich, B., Savin, A., Stoll, H., & Preuss, H. (1989). Results obtained with the correlation energy density functionals of Becke and Lee, Yang and Parr. *Chemical Physics Letters*, 157, 200–206. [https://doi.org/10.1016/0009-2614\(89\)87234-3](https://doi.org/10.1016/0009-2614(89)87234-3).
- 31 Koopmans, T. (1934). über Die Zuordnung Von Wellenfunktionen Und Eigenwerten Zu Den Einzelnen Elektronen Eines Atoms. *Physica*, 1, 104–113. [https://doi.org/10.1016/S0031-8914\(34\)90011-2](https://doi.org/10.1016/S0031-8914(34)90011-2)
- 32 Marenich, V., Cramer, C.J., & Truhlar, D.G. (2009). Universal solvation model based on solute electron density and a continuum model of the solvent defined by the bulk dielectric constant and atomic surface tensions. *The Journal of Physical Chemistry B*, 113(18), 6378–6396. <https://doi.org/10.1021/jp810292n>.

- 33 Miertus, S., Scrocco, E., & Tomasi, J. (1981). Electrostatic interaction of a solute with a continuum. A direct utilization of AB initio molecular potentials for the prevision of solvent effects. *Chemical Physics*, 55(1), 117–129. [https://doi.org/10.1016/0301-0104\(81\)85090-2](https://doi.org/10.1016/0301-0104(81)85090-2).
- 34 Mennucci, B. (2012). Polarizable continuum model. *Wiley interdisciplinary reviews: Computational Molecular Science*, 2(3), 386–404. <https://doi.org/10.1002/wcms.1086>.
- 35 Chalasiński, G., & Szczesniak, M.M. (1994). Origins of structure and energetics of van der Waals clusters from ab initio calculations. *Chemical Reviews*, 94, 1723–1765. <https://doi.org/10.1021/cr00031a001>.
- 36 Galano A., & Idaboy J.R.A. (2006). A new approach to counterpoise correction to BSSE. *Journal of Computational Chemistry*, 27(11), 1203–1210. <https://doi.org/10.1002/jcc.20438>.
- 37 Ozdemir, M.C., Ozgün, B., & Aktan, E. (2019). 1-Aryl-3,5-dimethylpyrazolium based tunable protic ionic liquids (TPILs). *Journal of Molecular Structure*, 1180, 564–572. <https://doi.org/10.1016/j.molstruc.2018.12.027>.
- 38 Ektirici, S., Kurç, Ö., Jalilzadeh, M., Aşır, S., & Türkmen, D. (2022). Computational investigation of the monomer ratio and solvent environment for the complex formed between sulfamethoxazole and functional monomer methacrylic acid. *ACS Omega* 7, 17175–17184. <https://doi.org/10.1021/acsomega.2c00862>.
- 39 Sarma, R., Bhattacharyya, P.K., & Baruah, J.B. (2011). Short range interactions in molecular complexes of 1,4-benzenediboronic acid with aromatic N-oxides. *Computational and Theoretical Chemistry*, 963 141–147 <https://doi.org/10.1016/j.comptc.2010.10.020>.
- 40 Houshmand, F., Neckoudaria, H., & Baghdadic, M. (2018). Host-guest interaction in chitosan–MX (3-chloro-4-(dichloromethyl)-5-hydroxy-2(5H)-furanone) complexes in watersolution: Density Functional Study. *Asian Journal of Nanoscience and Materials*, 2(1), 49–65.
- 41 Deka, B.C., & Bhattacharyya, P.Kr. (2015). Understanding chitosan as a gene carrier: A DFT study. *Computational and Theoretical Chemistry*, 1051, 35–41 <http://dx.doi.org/10.1016/j.comptc.2014.10.023>.
- 42 Deka, B.C., & Bhattacharyya, P.Kr. (2016). Response of chitosan–nucleobase interaction toward external perturbations: A computational study. *Computational and Theoretical Chemistry*, 1078, 72–80. <http://dx.doi.org/10.1016/j.comptc.2015.12.016>.
- 43 Jeremić, S., Tran, H., Marković, Z., Ngo, T.C., & Dao, D.Q. (2018). Insight into interaction properties between mercury and lead cations with chitosan and chitin: Density functional theory studies. *Computational and Theoretical Chemistry*, 1138, 99–106. <https://doi.org/10.1016/j.comptc.2018.06.010>.
- 44 Anchique, L., Alcázar, J.J., Ramos-Hernandez, A., Méndez-Lopez, M., Mora, J.R., Rangel, N., Paz, J.L., & Márquez, E. (2021). Predicting the Adsorption of Amoxicillin and Ibuprofen on Chitosan and Graphene Oxide Materials: A Density Functional Theory Study. *Polymers*, 13(10), 1620. <https://doi.org/10.3390/polym13101620>.

И.Н. Нұрғалиев

Хитозан аскорбат нанобөлшектерінің құрылымын DFT зерттеу

Соңғы жылдары хитозан (ХЗ) нанобөлшектерін нанотасымалдаушылар ретінде пайдалану олардың биоыдырағыштығына, биоүйлесімділігіне және уытты еместігіне байланысты көп көңіл бөлінуде. Құрамында препараттар, дәмдер, ферменттер және микробқақарсы агенттері бар ХЗ нанобөлшектері өз белсенділігін сақтай алады. Мұндай нанобөлшектер аскорбин қышқылының (АҚ) тұрақтануын ынталандырып, бақыланатын босатуды жақсарта алады. Бұл зерттеу хитозан аскорбатының нанокұрылымының (ХАН) түзілуі кезінде тығыздық функционалдық теориясы (DFT) арқылы ХЗ мономерінің АҚ және натрий-триполифосфатымен (ТПФ) өзара әрекеттесуін зерттейді. Қолданыстағы нәтижелер негізінде кешендерден түзілген ХЗ мономері донорлық-акцепторлық әрекеттесу есебінен пайда болады, ол есептеулер бойынша барлық қарастырылатын әрекеттесулерде энергетикалық жағынан қолайлы. Жақын қашықтықта өзара әрекеттесу энергиялары бар протонның тасымалдануы анықталды: сулы фазадағы ХЗ-АҚ (–6,82 ккал/моль), ХЗ-ТПФ (–4,56 ккал/моль). Бұл ХАН түзілу процесінде көп жағдайда донорлық-акцепторлық байланыстың түзілуі АҚ энол тобымен ХЗ амин топтары және ТПФ-мен ХЗ салыстырмалы координациясы арасында жүретінін көрсетеді. Сулы фазаның енгізілуі өзара әрекеттесу энергиясының төмендеуіне әкелді. Байланыс түрлеріне (өзара әрекеттесу энергиясы) нәтижелер негізінде олардың ХАН түзілу процесіне әсер етуінің қарапайым механизмі ұсынылған.

Кілт сөздер: хитозан, аскорбин қышқылы, натрий триполифосфаты, хитозан аскорбаты, нанобөлшектер, модельдеу.

И.Н. Нурғалиев

DFT исследование структуры наночастиц аскорбата хитозана

В последние годы большое внимание уделяется использованию наночастиц хитозана (ХЗ) в качестве наноносителей в связи с их биоразлагаемостью, биосовместимостью и нетоксичностью. Наночастицы ХЗ, содержащие лекарства, ароматизаторы, ферменты и противомикробные агенты, могут сохранять свою активность. Такие наночастицы могут стимулировать стабилизацию аскорбиновой кислоты (АК) и улучшать контролируемое высвобождение. В этой статье исследовано взаимодействие мономера ХЗ с АК и триполифосфатом натрия (ТПФ) с помощью теории функционала плотности (DFT) при формировании наноструктуры аскорбата хитозана (НАХ). На основании имеющихся результатов образования мономера ХС из комплексов происходит за счет донорно-акцепторного взаимодействия, которое, согласно расчетам, является энергетически выгодным во всех рассмотренных взаимодействиях. На близком расстоянии идентифицирован перенос протона с энергиями взаимодействия: ХЗ-АК (-6,82 ккал/моль), ХЗ-ТПФ (-4,56 ккал/моль) в водной фазе, что свидетельствует о том, что в процессе образования НАХ в большинстве случаев происходит образование донорно-акцепторной связи между аминогруппами ХЗ с енольной группой АК и относительная координация ХЗ с ТПФ. Введение водной фазы привело к падению энергии взаимодействия. На основании полученных результатов для типов связей (энергий взаимодействия) авторами предложен простой механизм их влияния на процесс формирования НАХ.

Ключевые слова: хитозан, аскорбиновая кислота, триполифосфат натрия, аскорбат хитозан, наночастицы, моделирование.

Information about the author*

Nurgaliev, Inar Nakipovich (*corresponding author*) — Doctor of Sciences in Physics and Mathematics, Head of the Laboratory of Theoretical Foundations of Polymer Chemistry and Physics, Institute of Chemistry and Physics of Polymers of the Academy of Sciences of the Republic of Uzbekistan, A. Kadyri street, 7 b, 100128, Tashkent, Uzbekistan; e-mail: ilnarvodnik@gmail.com; <https://orcid.org/0000-0002-6983-4375>

*The author's name is presented in the order: *Last Name, First and Middle Names*